ARTICLE OPEN

Check for updates

Quantum anomalous semimetals

Bo Fu 10 Jin-Yu Zou 1, Zi-Ang Hu 1, Huan-Wen Wang 10 and Shun-Qing Shen 10 Nen 10 Shen 10 Nen 10 Ne

The topological states of matter and topological materials have been attracting extensive interests as one of the frontier topics in condensed matter physics and materials science since the discovery of quantum Hall effect in 1980s. So far all the topological phases such as integer quantum Hall effect and topological insulators are characterized by integer topological invariants. None is a half integer or fractional. Here we propose a type of semimetals which hosts a single cone of Wilson fermions. The Wilson fermions possess linear dispersion near the Dirac point, but break the chiral or parity symmetry such that an unpaired Dirac cone can be realized on a lattice. In order to avoid the fermion doubling problem, the chiral symmetry or parity symmetry must be broken explicitly if the hermiticity, locality and translational invariance all hold. We find that the system can be classified by the relative homotopy group, and a half-integer topological invariant. We term the nontrivial quantum phase as quantum anomalous semimetal. The work opens the door towards exploring novel states of matter with fractional topological charge.

npj Quantum Materials (2022)7:94; https://doi.org/10.1038/s41535-022-00503-0

INTRODUCTION

Discovery of quantum Hall effect in 1980s opened an avenue to explore the topological states of matter and topological materials in condensed matter physics and materials science¹. The topological insulators and superconductors are classified as a state of matter according to the topology of band structure and are characterized by the Z and Z_2 topological invariants²⁻⁷, which determine the existence of the boundary states around the systems according to the bulk-boundary correspondence^{3,4}. Some topological metals and semimetals were also discovered to possess the Fermi arcs on the surface of the systems^{8–14}. However, so far all the discovered topological phases of matter and the topological materials are characterized by a nonzero integer. None of the topological invariant is a half-integer or fractional 15,16. The Nielsen-Ninomiya or fermion doubling theorem states that a single gapless Dirac fermion cannot be constructed on a regular lattice in even space-time dimensions while preserving all of the symmetries: translation invariance, chiral symmetry, locality, and hermiticity^{17,18}. By sacrificing one of the presuppositions, unpaired massless Dirac fermion can be formulated to get rid of the doublers. The chiral anomaly, one of the fundamental physics in quantum field theory, is closely related to the theorem. In odd space-time dimensions, the fermion doubling phenomenon in two spatial dimensions is intimately tied to another quantum anomaly, the so-called parity anomaly, which can be viewed as the analog to chiral anomaly in even space-time dimensions. Here we propose a topological state of matter, termed "quantum anomalous semimetal" to emphasize its close relation to quantum anomalies. This phase hosts the Wilson fermions instead of the Dirac fermions. The gapless Wilson fermions break the chiral or parity symmetry at generic momenta, and can be realized on lattices. It is found that the topological phase is classified by the relative homotopy group and characterized by a half-integer topological invariant. The half-integer topological invariant leads to a fractional electric and electromagnetic polarization in one and three dimensions¹⁹, and half-quantized Hall conductance in two and four dimensions with no well-defined boundary states²⁰, forming a distinct bulk-boundary correspondence from the gapped topological phase. An explicit consequence in the one-dimensional (1D) phase is the prediction of the transfer of one half of elementary charge e/2 in a topological charge pumping, which demonstrates the distinction of the phase to all other existing topological phases and materials.

RESULTS

Model and Wilson fermions

The massless Wilson fermions can be realized as a consequence of fermion regularization on a lattice, which can be described by the modified Dirac equation on a d-dimensional hyper-cubic lattice 6,18,21,22 .

$$H = \sum_{i=1}^{d} \left(\frac{\hbar v}{a} \sin k_i a \alpha_i - \frac{4b}{a^2} \sin^2 \frac{k_i a}{2} \beta \right) \tag{1}$$

with the lattice space a and effective velocity v where a_i and β are the Dirac matrices (See Methods). Its conduction band and valence band $E_{\pm}=\pm\sqrt{\sum_{i=0}^df_i^2(\mathbf{k})}$ with $f_0(\mathbf{k})=-\frac{4b}{a^2}\sum_{i=1}^d\sin^2\frac{k_ia}{2}$ and $f_i(\mathbf{k}) = \frac{\hbar v}{a} \sin k_i a$ (i = 1, ..., d) touches at $\mathbf{k} = 0$ to form a single Dirac cone of massless fermions (See Fig. 1a and b). A continuous model is valid by taking $\sin k_i a \simeq k_i a$ and also used in the following. In the case of d = 1, 3, it is known that the chiral symmetry is broken explicitly, in which the chirality operator $\mathcal{C}=$ $e^{-i\frac{\pi}{4}(d-1)}\prod_{i=1}^{d} \alpha_i$ does not commute with β . The Hamiltonian also exhibits a global sublattice symmetry, $\Gamma H\Gamma^{-1} = -H$ with $\Gamma = e^{-i\frac{\pi}{4}(d+1)}\beta \prod_{i=1}^{d} \alpha_i$. In the case of d=2, the parity operator is defined as $\mathcal{P} = \alpha_1 \hat{M}$ and under \hat{M} : $x \to x$ and $y \to -y^{23}$. The b term changes its sign under ${\cal P}$ and breaks the parity symmetry explicitly. Thus the Wilson fermions break the chiral or parity symmetry explicitly and avoid fermion doubling problem¹⁸. The symmetry breaking term becomes irrelavant and the symmetry is restored when $k_i \rightarrow 0$ near the degenerate point. This symmetry broken term plays a crucial role in the continuum limit and ensures the quantum anomaly is correctly reproduced 18,24. In the lattice gauge theory 18,24, any lattice discretization of the action with the following properties: (i) has the correct continuum limit, (ii) is gauge invariant, (iii) the Dirac operator is local, and (iv)

¹Department of Physics, The University of Hong Kong, Pokfulam Road, Hong Kong, China. [™]email: sshen@hku.hk



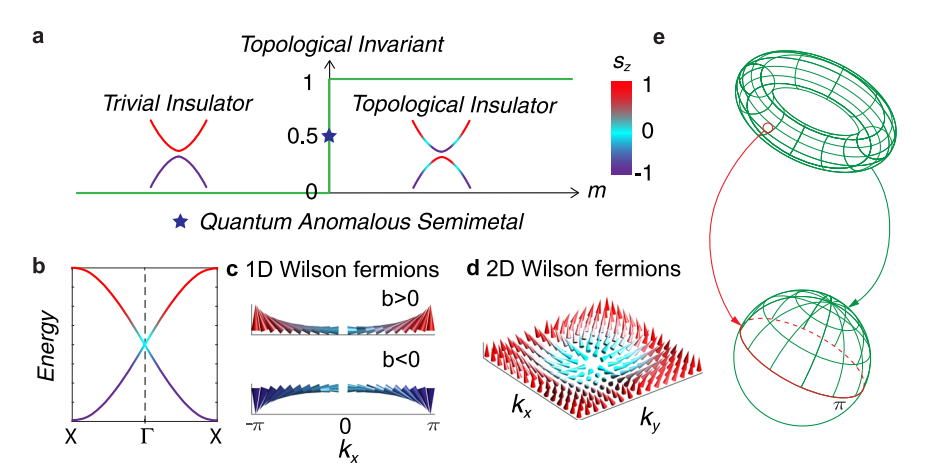


Fig. 1 Quantum anomalous semimetal. a The phase diagram and topological invariant of trivial insulator, quantum anomalous semimetal and topological insulator. **b** The dispersion of the Wilson fermions along the wave vector k_x and keeping all other $k_i = 0$. **c** The spin texture of 1D Wilson fermions. d The spin texture of 2D Wilson fermions. e The relative homotopy group mapping of band structure and spin texture of the parity anomalous semimetal. The whole torus on the first Brillouin zone maps to the semi-Bloch sphere (green line) and the small loop around crossing point to the equator of the Bloch sphere (red line).

absence of species doubling, reproduces the quantum anomaly in the continuum limit. Therefore, the fermion doubling phenomenon is intimately tied to quantum anomaly, i.e. the chiral anomaly for $d = 1, 3^{25,26}$ and the parity anomaly for $d = 2, 4^{27,28}$.

Classification of relative homotopy group

In the d-dimensional space, the Brillouin zone is topologically equivalent to a torus: $\mathbf{k} \in T^d$. Assume that the band crossing occurs at a single point in the momentum space {w} which serves as the "monopole" of the gauge field. To present a homotopy classification, we need to remove the degenerate point to avoid the singularity, which will change the topology of the Brillouin zone. We assume there are n occupied and m unoccupied Bloch bands for each momentum. On the complement $T^d \setminus \{\mathbf{w}\}$, one can define the Q-matrix $Q(\mathbf{k}) = 2P(\mathbf{k}) - I$ in terms of the projection operator $P(\mathbf{k}) = \sum_{a=1}^{n} |u_a(\mathbf{k})\rangle \langle u_a(\mathbf{k})|$, where $|u_a(\mathbf{k})\rangle$ are the occupied Bloch wave-functions. I is a $(m+n) \times (m+n)$ identity matrix. For a given system, $Q(\mathbf{k})$ defines a continuous map from the Brillouin zone $T^d \setminus \{\mathbf{w}\}$ to a specific topological manifold M, such that the Brillouin zone boundary surrounding the degenerate point ($\cong S^{d-1}$) is mapped to a submanifold $X \subset M$ (see an example in two dimensions as illustrated in Fig. 1e). Mathematically, the classification of topological semimetal phases is equivalent to distinguish distinct classes for all such mappings which are given by the relative homotopy group $\pi_d(M, X)^{29,30}$. In the following, we will identify the topological invariants with elements of the relative homotogy group for quantum anomalous semimetals in even (odd) spatial dimensions that parity (chiral) symmetry is broken for generic momenta but restored surrounding the degenerate point.

In even spatial dimensions, we consider the Hamiltonian that has no constraint other than being Hermitian and the translational symmetry. The Q-matrix thus defines a map from $T^d \setminus \{\mathbf{w}\}$ into the the complex Grassmannian $G_{m,m+n}(\mathbb{C}) = \frac{U(m+n)}{U(m) \times U(n)}$. The topological invariants characterizing distinct topological phases in this symmetry class are the first Chern number v_{2D} and second Chern number v_{4D} for two and four dimensions, respectively ^{15,22}. On the infinitesimal boundary surrounding the degenerate point, the parity symmetry is restored that the space of Q is restricted to U(n). By using the exact sequence²⁹, the relative homotopy group can be derived as: $\pi_d[G_{m,m+n}(\mathbb{C}),U(n)]\simeq \mathbb{Z}\oplus \mathbb{Z}$. There are two integers (N_1, N_2) characterizing the relative homotopy group which maps the Brillouin zone to the target space with its boundary to a specific submanifold. The Stokes theorem enables us to relate the topological invariants $v_{2D/4D}$ with these two integers, $v_{2D/4D} = N_1 + N_2/2$. As shown in Methods, by using Stokes theorem, $v_{2D/4D}$ can be separated into two parts: i) the winding number of a unitary matrix q which is an integer corresponding to N_1 , ii) one dimensional Berry connection integral P_1 or the Chern-Simons 3-form integral P_3 over the boundary surrounding the degenerate point. In general, $P_{1,3}$ can take any values within (-0.5, 0.5] without symmetry constraint. If the parity symmetry is further imposed on this boundary, the eigenstates of the Hamiltonian at **k** and \hat{M} **k** must be related by a unitary gauge transformation U. Consequently, the integral $P_{1,3}$ over this boundary is only one half of the winding number of U which corresponds to the second integer N_2 .

In odd spatial dimensions, we restrict our discussions in systems with sublattice symmetry (which requires m = n) which indicates that we can find a unitary matrix Γ anticommuting with the Hamiltonian, $\Gamma H \Gamma^{-1} = -H$. As a consequence, the Q-matrix can be brought into an off-diagonalized form with the off-diagonal component as $q(\mathbf{k})$ which defines a map from the Brillouin zone onto U(n). In this case, a winding number $w_{1D/3D}$ can be defined to characterize distinct topological classes. The restored chiral symmetry around the degenerate point further restricts $q(\mathbf{k}) \in$ $G_{a,n}(\mathbb{C})$ with $a \le n$ on the boundary of the Brillouin zone. The chiral anomalous semimetal is then classified by the relative homotopy group $\pi_d[U(n), G_{a,n}(\mathbb{C})] \simeq \mathbb{Z} \oplus \mathbb{Z}$ with two integers (N_1, N_2) . In 1D, N_1 counts the integer number of times that the argument of det[q(k)] varies along the path and N_2 indicates the monopole charge of the degenerate point. w_{1D} measures the argument variation of det[q(k)] along an open path divided by 2π . Due to the constraint of chiral symmetry, the arguments of the beginning and end points can only take two values 0 or π (modulo 2π). The difference of the arguments between these two points divided by π tracks the monopole charge. Hence, N_2 only gives half-integer contribution to the winding number. In 3D, w_{3D} can be converted to the integration over the boundary surrounding the degenerate point by utilizing the Stokes theorem as shown in Methods. With additional chiral symmetry on the boundary, this integral is reduced to the Berry curvature flux integral divided by 4π which is half of the monopole charge N_2 . Consequently, the winding number for the chiral anomalous semimetals in one and three dimensions can be obtained as $W_{1D/3D} = N_1 + \frac{1}{2}N_2$.

The existing classification theory of semimetals is based on the properties of the band structure near the crossing points¹⁶. For quantum anomalous semimetal, there are two topological integers to classify the matter, as given by the relative homotopy group. One characterizes the topology of the bands on the sphere S^{d-1} surrounding the crossing point and the other one characterizes the bands on the high energy scale. The quantum anomalous semimetals here host the massless Wilson fermions instead of the conventional Dirac fermions. The two types of fermions are similar near the crossing point but distinctly different at higher energy scales. The gapless Wilson fermions provide the simplest example of the quantum anomalous semimetals in various dimensions since the b term vanishes in the vicinity of the degenerate point. The topological invariant for gapless Wilson fermions is simply one half, $-\frac{1}{2} \operatorname{sgn}(b)$, which only depends on the sign of the symmetry broken coefficient b.

In the language of the tenfold-way of Altland-Zirnbauer symmetry classes 15,16,31 , in even spatial dimensions (parity anomalous semimetals), the system on manifold M belongs to the symmetry class A and on X belongs to the symmetry class AllI. In odd spatial dimensions (chiral anomalous semimetals), the system on manifold M belongs to the symmetry class AllI and on X belongs to class A. The homotopy groups in A and AllI form a 2-Bott period, i.e. A is nontrivial (trivial) in even (odd) dimensions, AllI is nontrivial (trivial) in odd (even) dimensions. This property leads to the result of the relative homotopy group $\mathbb{Z} \oplus \mathbb{Z}$. The Stokes theorem can apply between A and AllI and map the two integers to a half integer. Here we restrict our discussion on A and AllI because of the symmetries of quantum anomalous semimetal. The topological semimetal phase characterized by a half integer topological invariant in the other eightfold symmetry classes which form a 8-Bott period may need further study.

Spin texture interpretation of the half quantized topological invariants

We can take the Wilson fermions as examples to present the physical interpretation of the half-quantized topological invariants. We first discuss the half quantization of the winding number for 1D Wilson fermions. The Hamiltonian for 1D Wilson fermions can be expressed as $H_{1D} = \mathbf{f}(k) \cdot \boldsymbol{\sigma}$ with a vector $\mathbf{f} = (f_1(k), f_2(k), 0)$. As the name suggests, the winding number w_{1D} counts the number of times that the vector \mathbf{f} rotates around the origin as kvaries across the full Brillouin zone. The direction of the pseudospin vector on the Bloch sphere is $\hat{\mathbf{f}} = \frac{\mathbf{f}}{|\mathbf{f}|}$ as shown in Fig. 1c. Due to the presence of a sublattice symmetry of the bulk Hamiltonian, the pseudo-spin is forced to evolve on the equator of the Bloch sphere. For gapless Wilson fermions, the band gap vanishes at a specific momentum $\mathbf{f}(k_0) = \mathbf{0}$ where the pseudospin vector is ill-defined. The winding path of **f** will go through the origin at the gap closing point. The winding number is defined by $w_{1D} = \int \frac{dk}{2\pi} (\hat{f}_2 \partial_k \hat{f}_1 - \hat{f}_1 \partial_k \hat{f}_2)$. By removing the degenerate point, the reciprocal lattice vector space is no longer a closed path but an open segment with two end points. The additional chiral symmetry at the end points requires the directions of the pseudospin can only have the azimuthal angles as 0 or π . Once the locations of the two end points of the mapping fixed, the whole mapping **f** from the Brillouin zone are uniquely determined. With the sublattice symmetry and chiral symmetry at the degenerate point preserved, two mappings with different winding numbers can not be continuously deformed to other. The corresponding images of **f** wind around the circumference of the equator with half integer times. Consequently, we find that if chiral symmetry can be restored in the vicinity of the degenerate point, the winding number can still be well defined and quantized as a half integer.

This half-integer topological invariant for 2D Wilson fermions can also be understood by checking the winding number of mapping from the Brillouin zone to the Bloch sphere (Fig. 1e), $v_{2D} = \int \frac{d^2\mathbf{k}}{4\pi} \hat{\mathbf{f}} \cdot \left(\frac{\partial \hat{\mathbf{f}}}{\partial k_x} \times \frac{\partial \hat{\mathbf{f}}}{\partial k_y} \right) \text{ where } \hat{\mathbf{f}} = \mathbf{f}/|\mathbf{f}| \text{ with } \mathbf{f} = (f_1(\mathbf{k}), f_2(\mathbf{k}), f_3(\mathbf{k})).$ Physically, the unit vector $\hat{\mathbf{f}}$ represents the orientation of the

pseudo-spin associated with the eigenvector of the valence band. The additional parity symmetry around the boundary of the degenerate point will constrain $\hat{\mathbf{f}}$ to the equator. The pseudo-spin texture has the configuration shown as Fig. 1d which sweeps the upper or lower hemisphere depending on the sign of b. Hence, the topological invariant for 2D Wilson fermion can only take the half-integer values.

1D solvable model and topological half-charge pumping

For a periodically driven quantum two-level system, if the energy gap remains open, the final state evolves back to the initial one during a cyclic adiabatic process, the accumulated geometric phase is gauge invariant and experimentally measurable³². Geometric phases are key to understanding numerous physical effects, such as the electric polarization^{33,34} and anyonic fractional statistics³⁵. The topological invariants can be expressed in terms of these geometric phases which characterize the parallel transport of the ground state upon cyclic changes of system parameters (time t or wave vector k in the crystal band)³⁶. The time evolution of the two level system also reveals the topological property of the massless Wilson fermions. Here, we consider a solvable two-level system,

$$H_{1D}(t) = \frac{\hbar\omega_0}{2}\sin\omega t\sigma_x + \hbar\omega_0\sin^2\frac{\omega t}{2}\sigma_y, \tag{2}$$

which is periodic with a time $T(=2\pi/\omega)$, $H_{1D}(t+T)=H_{1D}(t)$. Eq. (2) is equivalent to the Hamiltonian (1) in 1D if ωt is replcaed by ka. The time evolution of this system is governed by the Schrodinger equation $i\hbar \frac{\partial \Psi(t)}{\partial t} = H(t)\Psi(t)$. The instantaneous energy eigenvalues are $E_\chi = \chi\hbar\omega_0 \sin\frac{\omega t}{2}$ with $\chi=\pm 1$. The two bands cross at time t=0 or T. The model possesses the glide reflection symmetry $\mathcal{G}(\omega t) = \begin{pmatrix} 0 & e^{-i\omega t} \\ 1 & 0 \end{pmatrix}$ such that $\mathcal{G}(\omega t)H_{1D}(t)\mathcal{G}^{-1}(\omega t) = H_{1D}(t)$. The

symmetry generator has the relation $\mathcal{G}^2(\omega t) = e^{-i\omega t}$, and its eigenvalues are $\chi e^{-i\omega t/2}$. Using the eigenstates of $\mathcal{G}(\omega t)$ as the basis, and solving the time-dependent Schrodinger equation, it is found that, in the adiabatic condition of $a = 8\omega_0/\omega \rightarrow +\infty$ that the system varies with time very slowly comparing with the band width $\hbar\omega_0$, the state is always stuck to the eigenstate of $\mathcal{G}(\omega t)$, i.e., the adiabatic theorem is still valid for this gapless system protected by the glide reflection symmetry (See Section "Onedimensional time-dependent model" in Supplementary Materials for more details). Consequently, the system evolves back to the initial state and the Berry phase π is gained after two periods of time, $\Psi(t=2T)=e^{i\pi}\Psi(t=0)$ as shown in Fig. 2a. At t=T, $\Psi(t=T)=-i\sigma_z e^{-i\frac{\alpha}{2}\sigma_x}\Psi(t=0).$ The phase α is attributed to the dynamic phase of of the system. If the initial state is one eigenstate of $\mathcal{G}(0)$, then at t = T it will evolve into another eigenstate of $\mathcal{G}(0)$. For a large but finite α the transition probability to the initial state at t = T is found to be $\frac{4}{\alpha n'}$, which approaches zero in the adiabatic condition. This reflects the non-Abelian topological property of the 1D system^{37,38}.

Furthermore, a striking feature of 1D Wilson fermions is a realization of the transfer of one half of elementary charge e/2 in a very slow and periodical modulation in time. The Thouless charge pumping^{39,40} was first proposed for a gapped system, in which the transferred charge is always an integer of elementary charge in an adiabatic cyclic evolution, and was observed experimentally in recent years^{41,42}. A half-quantized pumping rate in a quantum spin driven by two-harmonic incommensurate drives was proposed recently⁴³. Here the quantum anomaly of massless Wilson fermions makes it possible to realize a half-charge transfer in one periodic modulation in time. Let us consider a 1D tight-binding Hamiltonian in a time dependent modulation as shown in

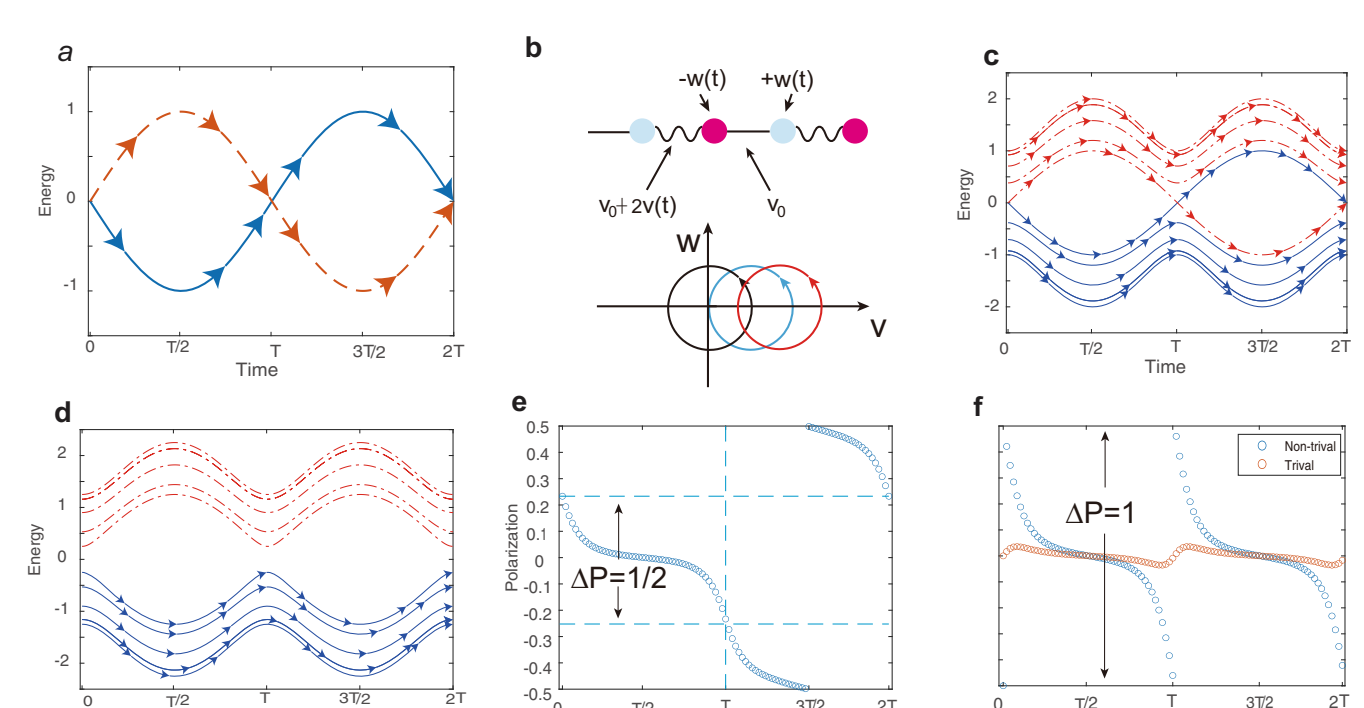


Fig. 2 Topological half-charge pumping. a The two-period time evolution in the two-level system. b The sketch of a half-charge pumping chain with $v(t) = v_0 \sin^2 \frac{\omega t}{2}$ and $w(t) = w_0 \sin^2 \frac{m t}{T}$ and the cyclic evolution in v-w space. The black and red circles mean for the topologically nontrivial case $v(t) = -\frac{v_0}{2} + v_0 \sin^2 \frac{\omega t}{2}$ and trivial case $v(t) = m + v_0 \sin^2 \frac{\omega t}{2}$ with m > 0. c The energy dispersion for the gapless one-dimensional chain in Eq. (3) in two time period T. d The energy dispersion for the gapped one-dimensional chain in Eq. (3) with a nonzero mass in $v(t) = m + v_0 \sin^2 \frac{\omega t}{2}$ in two time period T. e Electric polarization as a function of t in two time period T for the gapless one dimensional chain. f Electric polarization as a function of t in one time period T for the gapped cases of $v(t) = m + v_0 \sin^2 \frac{\omega t}{2}$ and $v(t) = -\frac{v_0}{2} + v_0 \sin^2 \frac{\omega t}{2}$.

Fig. 2b (upper panel),

$$H(t) = \sum_{n} \left[(v(t) + (v_0 + v(t))(-1)^n) c_n^{\dagger} c_{n+1} + h.c. + w(t)(-1)^n c_n^{\dagger} c_n \right]$$
(3)

where v_0 is real constant. The modulating hoping strength $v(t)=v_0\sin^2\frac{\omega t}{2}$ and potential $w(t)=w_0\sin(\omega t)$ form a cyclic evolution in the parameter space shown in Fig. 2b (lower panel) such that the Hamiltonian is also periodic in time: H(t)=H(t+T). By transforming into momentum space, Eq. (3) becomes $H(k,t)=w_0\sin(\omega t)\sigma_z+v_0\sin(ka)\sigma_y+2v_0(\sin^2\frac{k\alpha}{2}+\sin^2\frac{\omega t}{2})\sigma_x$. In two dimensional parameter space (k,t), it is equivalent to Eq. (1) in 2D up to a basis transformation. The energy evolution of the system in the adiabatic condition is plotted in Fig. 2c and d for the massless and massive cases. Only the two states around the zero energy evolve in the period of 2T, and swap their energy signs at t=T, and all other states evolve in the period of T as expected in the adiabatic evolution for an isolated system.

The charge that flows through the system during one period is given by $\Delta Q = \int_{-T/2}^{T/2} dt \, \frac{dP_x(t)}{dt}$ where P_x is the charge polarization defined as the shift of the electron center-of-mass position away from the lattice sites and is only well-defined modulo 1. The time dependence of P_x is evaluated by the many-body polarization formula using all instantaneous occupied states at time t^{34} . It can be formulated in terms of the expectation value of $P_x(t) = \frac{1}{2\pi} \mathrm{Im} \ln \langle \Phi(t) | e^{2\pi i \hat{x}/N} | \Phi(t) \rangle$ with $\hat{x} = \sum_n n c_n^{\dagger} c_n$ is the position operator. Here we consider the Hamiltonian in Eq. (3) on a ring with N sites. The time evolution of the energy spectrum in Eq. (3) with a periodical boundary condition for two period 2T is plotted in Fig. 2c. The band gap is closed at $t^* = 0$. For $t \neq t^*$, the system is fully gapped and the calculated polarization P_x is presented in Fig. 2e. The time evolution of the two-subbands system closest to

zero energy is governed by Eq. 2. Thus, $|\Phi(t)\rangle$ is the ground state during the period 0 < t < T and the first excited state for the period T < t < 2T, denoted by the blue lines in Fig. 2c. The total pumped charge in a single period T is given by $\Delta Q = -\frac{1}{2} \operatorname{sgn}(w_0)$, which equals the winding number around the band crossing point in the (1+1)-dimensional parameter space. As the fermion doubling problem has been circumvented, there is only a single gap closing time t^* in one period T, which guarantees the quantization of the total pumped charge ΔQ as a half-integer instead of an integer in a gapped system. This 2T periodicity of polarization evolution for quantum anomalous semimetal is completely different from the gapped cases that the energy gap remains open during a cyclic change of t as shown in Fig. 2d. As illustrated in Fig. 2f, the gapping of the quantum anomalous semimetal leads to two distinct spectrums of polarization which are indicated by red (trivial) and blue (nontrivial) circles and both exhibit a T periodicity.

Generalized bulk-boundary correspondence

The bulk-boundary correspondence lies at the heart of the topological phases. For example, in the quantum Hall effect the Chern number in quantum Hall conductivity means the number of the chiral edge states around the boundary 44 . The half-quantized Hall conductivity in a parity anomalous semimetal here does not mean the existence of one half of the edge state, but reveals the existence of chiral edge current although the energy band gap is closed. To this end, we evaluate the local density of states (LDOS) at the position near the two edges and the middle position of a strip of two-dimensional (2D) sample with a sufficient width to avoid the finite size effect. Along the *x*-direction, we take the periodic condition, and the wave vector k_x is a good quantum number. The corresponding tight-binding model for this strip

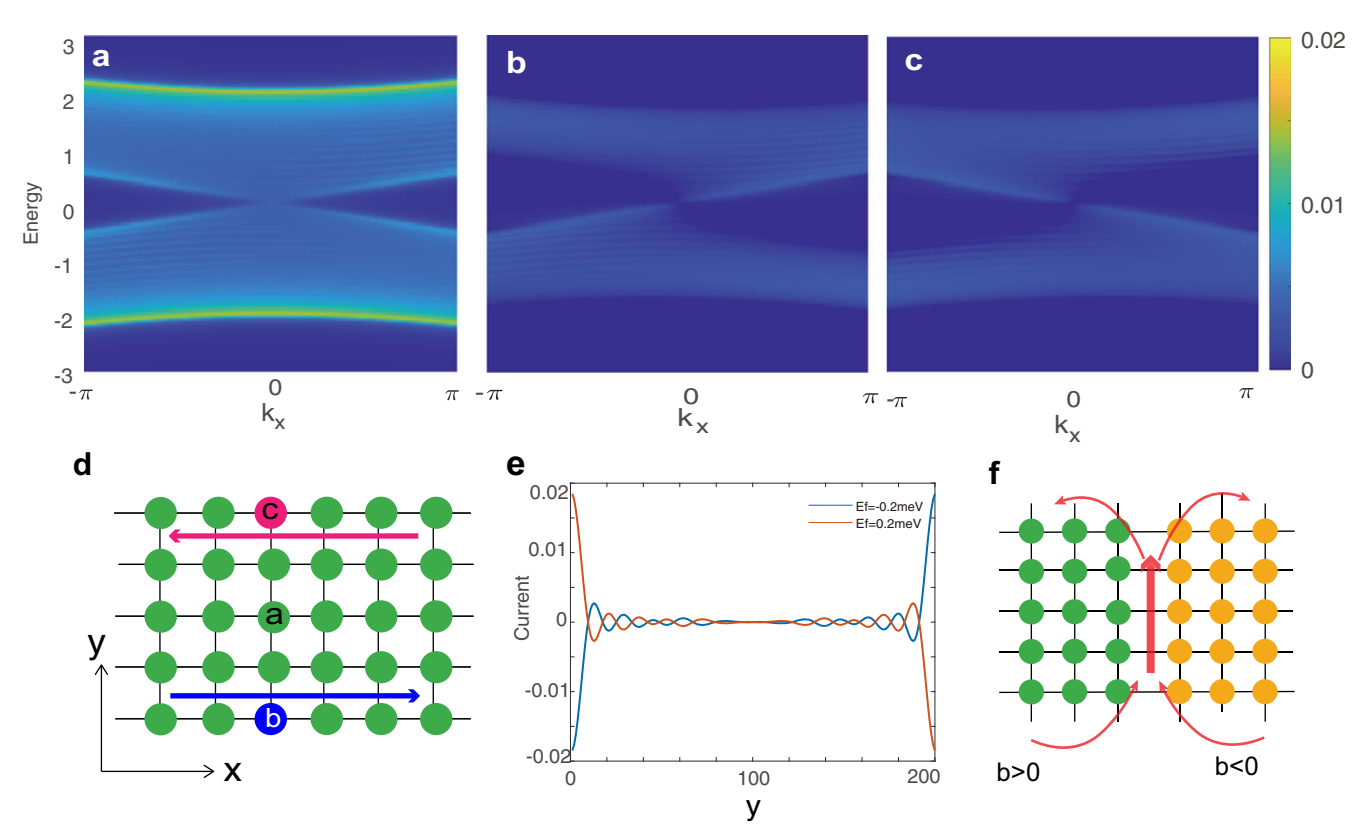


Fig. 3 The local density of states and edge current distribution in the absence of external field. a The local density of states at the middle of the sample. **b** The relative local density of states at the top edge (pink dot) $\rho_r(k_x, y = L_y)$. **c** The relative local density of states at the bottom edge (blue dot) $\rho_r(k_x, y = 1)$. The relative local density of states means that the contribution from bulk is already deducted, $\rho_r(k_x, 1) = \rho(k_x, 1) - \rho(k_x, L_y/2)$ and $\rho_r(k_x, L_y) = \rho(k_x, L_y/2)$. **d** A schematic of a stripe sample with the labelled positions for (**a**, **b**, and **c**). **e** The current density distribution for two different Fermi levels slight deviating from the half filling. **f** The Hall and longitudinal currents along the domain wall in two dimensions. Here $L_v = 200$, v = 1 and $b_0 = 0.5$.

structure can be found from the Eq. (1) as

$$H = \sum_{nk_x} c_{k_x,n}^{\dagger} \left(\frac{\hbar v}{a} \sin k_x a \sigma_x - \frac{2b}{a^2} (2 - \cos k_x a) \sigma_z \right) c_{k_x,n}$$

$$+ \left(\sum_{nk_x} c_{k_x,n-1}^{\dagger} \left(\frac{\hbar v}{2ai} \sigma_y - \frac{b}{a^2} \sigma_z \right) c_{k_x,n} + h.c. \right).$$

$$(4)$$

Then, the LDOS can be evaluated as a function of k_x and the position y, $\rho(k_x, y)^{45}$ as plotted in Fig. 3a, b and c, which positions are labelled schematically in Fig. 3d. At the middle of the sample, the LDOS $\rho(k_x, y = L_y/2)$ is even about k_x , which indicates that there is no pure current in the bulk without an external field. At the two points close to the edges y = 1 and L_v (L_v is the width of the stripe), the relative LDOS $\rho_r(k_x, 1)$ and $\rho_r(k_x, L_y)$ are plotted in Fig. 3b and c, in which the contribution of the bulk part has been deducted. We find that the nonzero relative LDOS emerges and maximizes at $E = \pm \hbar v k_x$ at the two edge positions y = 1 and L_v . This biased distribution in LDOS indicates that a chiral current lays at the edge of the sample. This current can be illuminated directly by calculating the many-body local current density $\langle v_x(y) \rangle$ of all occupied states along the sample, where $v_x(y) = \frac{1}{h} \frac{\partial H(k_x, y)}{\partial k_x}$. Current density distribution at two different chemical potentials are presented in Fig. 3e. Consequently a chiral current may circulate without well-defined edge states along the boundary in the absence of external field. This forms the bulk-edge correspondence in a quantum anomalous semimetal.

Formation of the bound state around the domain wall also provides an alternative way to demonstrate the bulk-boundary correspondence. We first consider a 1D static domain wall that the parameter b has a kink along the x direction., i.e.

 $b(x) = b_0 \text{sgn}(x)$. In addition to the extended bulk states, the exact solution demonstrate that there always exists a bound state of zero energy localized around the domain wall $\psi(x) =$

 $\chi_{y,1}/|\frac{\hbar v}{2b_0}|\exp(-|\hbar vx/b_0|)$ with χ_y the eigen spinor of $\sigma_{y,y}$ $\sigma_{y}\chi_{y}=\mathrm{sgn}(b_{0})\chi_{y}$. The result is analogous to the early theoretical prediction of domain wall fermions given by Jackiw and Rebbi in the context of relativistic field theory⁴⁶. However in the present situation, the bound state trapped around the domain wall between topologically distinct regions will coexist with the extended states in the bulk. The solution of the bound state can be generalized to two and three dimensions. In the 2D domain wall in Fig. 3f, the momentum $\hbar k_v$ is still conserved. One can obtain a solution of the chiral bound states along the domain wall with a linear dispersion $\textit{E} = \text{sgn}(\textit{b}_{0})\hbar\textit{vk}_{\textit{y}}$, which may carry one quantized conductance of e^2/h . These states are located near the domain wall, and decay exponentially away from the domain wall in space. Furthermore, in the three-dimensional (3D) case there exists a gapless Dirac cone of fermions with linear dispersion located at the interface (See Section "Solutions of the domain-wall bound state" in Supplementary Materials for more details). All these bound states coexist with the bulk states as the systems have no energy gap. The existence of the bound state is closely related to the fact that the difference of the topological invariants between the two sides of the domain wall is always equal to +1 or -1, although the topological invariants are one half. It can be viewed as an extension of the index theorem for gapped systems 16 to the gapless systems with fractional indices.



Quantum anomaly in a domain wall

Quantum anomaly provides a deep insight into the peculiar transport properties of the topological phase. To illustrate the quantum anomaly of Wilson fermions we continue to investigate the 2D domain wall in Fig. 3f that the parameter b has a kink along the x direction and is constant along y direction. The system is coupled to a weak electromagnetic potential A_{μ} via the minimal substitution rule (dictated by the gauge invariance). The Chern-Simons field theory provides a natural theoretical framework to describe the properties of the topological phases^{47–49}. The Chern-Simons term arises in the effective action of the gauge field A_{ij} from the fermionic fluctuations in Wilson fermion as a result of the violation of parity symmetry. The effective action far from the location of the wall (lies along the y direction) is $S_{\text{eff}}^{\text{CS}} =$ $\frac{1}{4\pi}\int d^3x n_c(b(x_1))\epsilon^{\mu\nu\lambda}A_{\mu}\partial_{\nu}A_{\lambda}$ with space-time coordinate $x^{\mu}=(t,x,y)$ and $e^{\mu\nu\lambda}$ Levi-Civita symbol that the Greek indices (μ , ν , etc.) run over all the space-time indices (0, 1, 2). For (2+1)D translational invariant system, the coupling constant n_c in Chern-Simons action is equal to the topological invariant v_{2D} . By taking the functional derivatives of $S_{\mathrm{eff}}^{\mathrm{CS}}$ with respect to A_{μ} , the current can be obtained as $\langle J_{\text{CS}}^{\mu} \rangle = \frac{1}{2\pi} n_c(b(x_1)) e^{\mu\nu\lambda} \partial_{\nu} \dot{A}_{\lambda} - \frac{1}{4\pi} \delta(x_1) e^{1\mu\lambda} A_{\lambda}$. However, this action is not invariant under the gauge transformation $A_u \rightarrow A_u + \partial_u \Phi(x)$ at the domain wall, because the domain-wall bound states are chiral which also has consistent chiral anomaly^{50,51}. The boundary action associated with the boundary excitations has to be included such that the total effective action is gauge invariant. Now we consider the electric field parallel to the domain wall as $E_1 = 0$, and $E_2 = E$. Then the Hall current of the anomalous Hall state $J_1 =$ $-\frac{e^2}{h}n_c(b(x_1))E$ flows towards the domain wall and the longitudinal current along the domain wall is $J_2 = \frac{e^2}{h}E$. Here we do not take into account the longitudinal minimal conductivity from the 2D massless fermions. The conductance along the domain wall is quantized. Here the bulk Hall coefficient $n_c = -\frac{1}{2} \operatorname{sgn}(b(x_1))$ is half-quantized and the Hall currents from both sides flow toward or outward the domain wall. The quantized charge current along the wall can be understood as a consequence of the convergence of two anomalous Hall currents because of the conservation of the total charge current. The boundary states suffer from the chiral anomaly as $\partial_{\mu}\langle J^{\mu}\rangle = -\frac{1}{2\pi}\epsilon^{\rho\lambda}\partial_{\rho}A_{\lambda}$ where the Greek indices only run over the space-time indices (0, 2), i.e. the charge conservation is broken at the domain wall since the current can leak into the bulk through the bulk quantum Hall effect. Thus the half-quantization of the bulk Hall conductance at the two sides of the domain wall is manifested as the quantization of the chiral anomaly coefficient along the domain wall, which is consistent with the solution of the chiral states in the previous section. This effect also reveals the bulk-edge correspondence in this topological phase.

DISCUSSION

The quantum anomalous semimetals can be realized in two alternative ways, one is the accidental band crossing and another is the band crossing protected by additional crystalline symmetries. At the critical transition point between the conventional and topological insulators, the accidental band crossing may give rise to the Wilson fermions by fine tuning the band gap, for example, the HgTe quantum well grown at a critical thickness where the band gap vanishes and the strain-controlled narrow gapped $ZrTe_5^{53}$. The topological phases may be stable against sufficient weak but short range electronic interactions and random mass at least for d=2 and 3 based on the scaling and renormalization group analysis.

Here we take a quasi-1D system as an example to discuss the stability of the band crossing and the evasion of fermion doubling problem by additional crystalline symmetry. Generally, the

symmetry-enforced band crossings can be movable at some high symmetry line or pinned at a particular high-symmetry point 13,5 In 1D, the movable band crossing can be protected by the nonsymmorphic crystal symmetry which is a combination of a point-group symmetry with a translation of a fractional Bravais lattice. For a biparticle system with glide mirror symmetry \overline{M}_{v} , the square of \overline{M}_{v} is a lattice translation of one unit cell. The bipartite lattice further possesses the sublattice symmetry when only the nearest neighbor hopping are included. Consequently, the energy eigenstates are actually the instantaneous eigenstates of \overline{M}_{v} . Upon shifting the momentum by one reciprocal lattice vector, the eigenvalues of \overline{M}_{v} remains unchanged, but the two energy branches must cross odd times in the Brillouin zone. One needs to go through the Brillouin zone twice to get back to the same eigenvalue. Therefore a global topological invariant w_{1D} can be introduced to characterizes the symmetry-enforced band crossing which measures the winding of the eigenvalue of \overline{M}_{ν} as going through the Brillouin zone. Section "Symmetry enforced band crossing" in Supplementary Materials shows additional details for the above discussion. By sacrificing the hermiticity, the single Dirac fermion can also be realized on lattice which is robust against the disorder⁵⁵. The quantum anomalous semimetal in 2D can be realized in semi-magnetic topological slab⁵⁶. Consider a time reversal invariant topological insulator slab, if the surface states are gapped by magnetic doping or proximity effect at one surface while the surface states at the opposite surface remain gapless, an unpaired gapless Dirac cone can be realized in this quasi-2D system. Finding a potential candidate in 3D remains a major challenge and we leave it for future research. A promising alternative way to realize the topological phase is in designed artificial systems, such as cold atoms, photonic/acoustic metamaterials, and circuit networks, which provide good platforms to simulate various topological phases in solid state physics.

METHODS

Dirac matrices in one, two, and three spatial dimensions

In one dimension, the matrices α_1 and β can be any two of the Pauli matrices, say $\alpha_1=\sigma_1$ and $\beta=\sigma_3$. In two dimensions, $\alpha_1=\sigma_1$, $\alpha_2=\sigma_2$ and $\beta=\sigma_3$. In three dimensions, the four Dirac matrices are $\alpha_i=\tau_1\sigma_i$ (i=1,2,3) and $\beta=\tau_3\sigma_0$. In four dimensions, the fourth alpha matrix is $\alpha_4=\tau_2\sigma_0$. Correspondingly, the five Dirac gamma matrices $\gamma^0=\beta=\tau_3\sigma_0$, $\gamma^i=\beta\alpha_i=i\tau_2\sigma_i$ and $\gamma^5=i\gamma^0\gamma^1\gamma^2\gamma^3=\tau_1\sigma_0$. Here τ_i and σ_i (i=1,2,3) are the Pauli matrices. τ_0 and σ_0 are the 2×2 identity matrices.

The classification of the relative homotopy group

For the manifold pair (M, A), where A is the sub-manifold of M, there is an exact sequence

$$\dots \to \pi_k(A) \xrightarrow{i_*} \pi_k(M) \xrightarrow{j_*} \pi_k(M, A) \xrightarrow{\partial_*} \pi_{k-1}(A) \xrightarrow{i_*} \pi_{k-1}(M) \xrightarrow{j_*} \pi_{k-1}(M, A) \to \dots$$
(5)

The holomorphic mappings i_* , j_* and ∂_* in the sequence satisfy that the image of each mapping equals the kernel of the next mapping. In the maintext, the manifold pair is $(G_{n,2n}(\mathbb{C}),U(n))$ for even spatial dimension and $(U(n),G_{a,n}(\mathbb{C}))$ for odd dimension. Notice that, for $n \geq (d+1)/2$ (d is the spatial dimension),

$$\pi_{j}[U(n)] = \begin{cases} 0, & j \in \text{even}, \\ \mathbb{Z}, & j \in \text{odd}; \end{cases}$$
 (6)

$$\pi_{j}[G_{n,2n}(\mathbb{C})] = \begin{cases} 0, & j \in \text{odd}, \\ \mathbb{Z}, & j \in \text{even}. \end{cases}$$
 (7)

We have the short exact sequence

$$0 \to \mathbb{Z} \to \pi_2[G_{n,2n}(\mathbb{C}),U(n)] \to \mathbb{Z} \to 0, \tag{8}$$

and

$$0 \to \mathbb{Z} \to \pi_{1,3}[U(n), G_{a,n}(\mathbb{C})] \to \mathbb{Z} \to 0. \tag{9}$$

According to the property of the short exact sequence²⁹, one yields $\pi_2[G_{n,2n}(\mathbb{C}),U(n)]\simeq \mathbb{Z}\oplus \mathbb{Z}$, and $\pi_{1,3}[U(n),G_{a,n}(\mathbb{C})]\simeq \mathbb{Z}\oplus \mathbb{Z}$.

Evaluation of topological invariants

Based on the analysis of relative homotopy group, we come to present the calculation of the topological invariants for the gapless Wilson fermions.

Topological invariants for odd dimensions. For odd spatial dimensions, we restrict our discussion in systems with the sublattice symmetry, which means that we can always find a unitary matrix Γ such that $\Gamma H\Gamma^{-1}=-H$. Then the Q- matrix can be brought into an off-diagonal form

$$Q(\mathbf{k}) = \begin{pmatrix} 0 & q(\mathbf{k}) \\ q^{\dagger}(\mathbf{k}) & 0 \end{pmatrix}. \tag{10}$$

After removing the degenerate point, we can use the spectral flattening technique to evaluate the winding number. In one and three dimensions, the winding numbers are given by^{15,57}

$$w_{1D} = i \int \frac{dk}{2\pi} \text{Tr}[q^{-1}(k)\partial_k q(k)]$$
(11)

and

$$w_{3D} = \int \frac{d^3 \mathbf{k}}{24\pi^2} \epsilon^{\alpha\beta\gamma} \text{ReTr}[q^{-1} \partial_{\alpha} q q^{-1} \partial_{\beta} q q^{-1} \partial_{\gamma} q], \tag{12}$$

respectively, where $e^{a\beta\gamma}$ is the Levi-Civita symbol with $a,\beta,\gamma=k_x$, k_y,k_z . Re denotes the real part, and Tr denotes the trace. In order to evaluate the winding number, we parameterize the off-diagonal matrix $q(\mathbf{k})$ as $q(\mathbf{k}) = \sum_n e^{i\beta_n(\mathbf{k})} |u_{n,\mathbf{k}}^R\rangle \langle u_{n,\mathbf{k}}^L|$ with $|u_{n,\mathbf{k}}^{R,L}\rangle$ the n-th right and left Bloch eigenstates satisfying $q(\mathbf{k})|u_{n,\mathbf{k}}^R\rangle = e^{i\beta_n(\mathbf{k})}|u_{n,\mathbf{k}}^R\rangle$, and $\langle u_{n,\mathbf{k}}^L|u_{n,\mathbf{k}}^R\rangle = \delta_{n,m}$. By performing the integral, the 1D winding number can be converted to the phase difference of two end points,

$$w_{1D} = i \int \frac{dk}{2\pi} \partial_k \text{Tr}[\ln q(k)] = \frac{i}{2\pi} [\ln \det(q^+) - \ln \det(q^-)] + N.$$
(1)

where $q^\pm=q(k_0\pm\delta)$ with δ is an infinitesimally positive number and k_0 as the band crossing point, N is an integer which is related to the homotopy group $\pi_1[U(m)]=Z$ classifying the maps from the Brillouin zone to $q(\mathbf{k})$. Near the two end points, the chiral symmetry is restored such that the q^\pm matrices are elements of U(m) and satisfy the hermitian condition $(q^\pm)^\dagger=q^\pm$. The eigenvalues of a hermitian and unitary matrix can only take the value of ± 1 . As a consequence, the winding number is reduced to the difference of the argument angles of the two end points,

$$W_{1D} = \frac{1}{2} \left(\sum_{n, \text{with } \theta_n^+ = \pi} 1 - \sum_{n, \text{with } \theta_n^- = \pi} 1 \right) + N.$$
 (14)

Thus the first term is a half of integer which are contributed by the two end points. Similarly, the 3D winding number reads

$$w_{3D} = \int \frac{d^3\mathbf{k}}{8\pi^2} \epsilon^{\alpha\beta\gamma} \mathrm{Re} \sum_{n,n'} \partial_{\gamma} \Big[\delta_{nn'} \vartheta_{n'}(\mathbf{k}) \mathcal{F}_{\alpha\beta}^{n'n'}(\mathbf{k}) + i \sin \vartheta_{n,n'}(\mathbf{k}) \mathcal{A}_{\alpha}^{n'n}(\mathbf{k}) \mathcal{A}_{\beta}^{nn'}(\mathbf{k}) \Big]$$

with $\vartheta_{n,n'}=\vartheta_n-\vartheta_{n'}$ and the Berry connection $\mathcal{A}_a^{nn'}(\mathbf{k})=$ $i\langle u^R_{n,\mathbf{k}}|\partial_\alpha u^L_{n',\mathbf{k}}\rangle$ and the Berry curvature $\mathcal{F}^{nn'}_{\alpha\beta}(\mathbf{k})=\partial_\alpha \mathcal{A}^{nn'}_\beta(\mathbf{k}) \partial_{\beta} \mathcal{A}_{\alpha}^{nn'}(\mathbf{k})$. This expression is a total derivative which only has a contribution on the boundaries. The degenerate point acts as the monopole of the Berry curvature in momentum space, thus the first term will yield a nontrivial contribution to w_{3D} . Since the chiral symmetry is restored around the degenerate point, the off-diagonal matrix $q(\mathbf{k})$ is a member of U(2m) which satisfies the hermitian condition $q^{\dagger}(\mathbf{k}) = q(\mathbf{k})$. The eigenvalues of $q(\mathbf{k})$ can be brought into two sectors with +1 and -1 values which have the argument angle as 0 and π respectively. We always have $\sin(\vartheta_{+-}) = 0$ at the boundary. Thus, the second term in the bracket of Eq. (15) vanishes and we only need to consider the first term. Only the bands with the -1 eigenvalues will contribution. By introducing the monopole charge associated with the crossing point, $v_{\text{Ch}} = \sum_{n, \text{with} \theta_n = \pi} \iint$ $\partial BZ \frac{dS}{2\pi} \hat{\mathbf{n}} \cdot \mathcal{F}^{nn}$, the winding number can be expressed as

$$w_{3D} = \frac{1}{2}v_{Ch} + N. {(16)}$$

For instance, for the massless Wilson fermions, the unitary matrix $\Gamma = \sigma_2$ in 1D and $\Gamma = \gamma^1 \gamma^2 \gamma^3$ in 3D. Consequently, both the 1D and 3D winding numbers are given by $w_{1D/3D} = -\frac{1}{2} \text{sgn}(b)$.

Topological invariants for even dimensions. In even spatial dimensions, the Chern number can be expressed in terms of the non-abelian Berry gauge field in momentum space. In order to figure out how the boundary of Brillouin zone modifies the topological invariants we express the first Chern number in 2D in the total derivative form as^{22,57},

$$v_{2D} = \int \frac{d^2k}{2\pi} \epsilon^{ij} \partial_i \text{Tr}[\mathcal{A}_j]. \tag{17}$$

The whole Brillouin zone $T^d\setminus \{\mathbf{w}\}$ can be divided into two patches, the inner (i) and outer (o) region, respectively, where the wave function $|u^{in}\rangle$ and $|u^{out}\rangle$ can be defined smoothly. Along the shared boundary (∂B) , the wave functions are connected by the gauge transformation $|u^{in}\rangle = g|u^{out}\rangle$ which yields $\mathcal{A}_i^{in} = g^{-1}\mathcal{A}_i^{out}g - ig^{-1}\partial_i g$ where g is a $n\times n$ unitary matrix. By using the Stokes' theorem, the integral of the Berry curvature over $T^d\setminus \{\mathbf{w}\}$ can be converted into the integrals over the boundaries (∂B) and $\partial \{T^2\setminus \{\mathbf{w}\}\}$,

$$v_{2D} = \frac{i}{2\pi} \int_{\partial B} dk \hat{n}_i e^{ij} \text{Tr}(g^{-1} \partial_i g) + P_1, \qquad (18)$$

where $\hat{\boldsymbol{n}}$ is the outward-pointing unit normal vector on the boundary, and $P_1 = \frac{1}{2\pi} \int_{\partial [T^2 \setminus \{\mathbf{w}\}]} dk \hat{n}_i e^{ij} \text{tr}[\mathcal{A}_j]$. The first term in Eq. (18) corresponds to the winding number along the boundary ∂B which is an integer. Consider the Hamiltonian $H(\mathbf{k})$ restores the parity symmetry near the degenerate point, i.e. $\mathcal{P}H(\mathbf{k})\mathcal{P}^{-1}=H(\hat{M}\mathbf{k})$, where \hat{M} is an operator in momentum space transforming $\mathbf{k} \to \hat{M}\mathbf{k} = (k_x, -k_y)$. Due to the parity symmetry (mirror symmetry in even spatial dimensions), the eigenstates of $H(\mathbf{k})$ at \mathbf{k} and $\hat{M}\mathbf{k}$ on the boundary $\partial [T^2 \setminus \{\mathbf{w}\}]$ must related by a gauge transformation: $\mathcal{P}|u_a(\mathbf{k})
angle =$ $\sum_b U_{ab}(\mathbf{k}) |u_b(\hat{M}\mathbf{k})\rangle$ where $U_{ab}(\mathbf{k})$ are the matrix elements of a unitary transformation acting on the space of the occupied bands. Accordingly, the Berry connection is transformed to $A_i(\mathbf{k}) = -iU^*(\mathbf{k})\partial_i U^T(\mathbf{k}) + \sum_i J_{ij} U^*(\mathbf{k}) A_i(\hat{M}\mathbf{k}) U^T(\mathbf{k})$, where * and T represent the complex conjugate and transpose, respectively and $J_{ij} = \partial (\hat{M} \mathbf{k})_i / \partial k_i$. The determinant of the Jacobian matrix J_{ij} equals -1. It follows that $2P_1 = \frac{i}{2\pi} \int_{\partial [T^2 \setminus \{\mathbf{w}\}]} dk \hat{n}_i \epsilon^{ij} \text{Tr}(U^{\dagger} \partial_i U)$ is an



integer. Thus the Chern number is

$$v_{2D} = N_1 + \frac{1}{2}N_2 \tag{19}$$

with N_1 and N_2 being integers.

Similarly, we can express the second Chern number in 4D $v_{4D} = \int \frac{d^4k}{23\pi^2} e^{ijkl} \text{Tr}[\mathcal{F}_{ij}\mathcal{F}_{kl}]$ as the total derivative form^{22,57}

$$v_{4D} = \int \frac{d^4k}{16\pi^2} \epsilon^{ijkl} \partial_i \text{Tr} \left[\left(\mathcal{F}_{jk} - \frac{1}{3} \left[\mathcal{A}_j, \mathcal{A}_k \right] \right) \mathcal{A}_l \right], \tag{20}$$

where the matrix elements of non-Abelian Berry connection and Berry curvature are defined as $\mathcal{A}_i^{ab}(\mathbf{k}) = i \langle u_a(\mathbf{k}) | \partial_i u_b(\mathbf{k}) \rangle$ and $\mathcal{F}_{ij}^{ab}(\mathbf{k}) = \partial_i \mathcal{A}_j^{ab}(\mathbf{k}) - \partial_j \mathcal{A}_i^{ab} + i [\mathcal{A}_i, \mathcal{A}_j]^{ab}$, respectively. Following the similar procedure in 2D, Eq. (20) can be converted into integrals over the boundaries (∂B and $\partial [T^2 \setminus \{\mathbf{w}\}]$),

$$v_{4D} = \frac{i}{24\pi^2} \int_{\partial B} d^3k \hat{n}_i \epsilon^{ijkl} \text{Tr}[(g^{-1} \partial_j g)(g^{-1} \partial_k g)(g^{-1} \partial_l g)] + P_3 \qquad (21)$$

where $P_3=\frac{1}{16\pi^2}\int_{\partial[T^4\setminus\{\mathbf{w}\}]}d^3k\hat{n}_i\epsilon^{ijkl}\mathrm{Tr}\big[\big(\mathcal{F}_{jk}-\frac{1}{3}\left[\mathcal{A}_j,\mathcal{A}_k\right]\big)\mathcal{A}_I\big]$ is the Chern-Simons 3-form integral over the boundary surrounding the degenerate point. The parity symmetry links two states on the boundary $\partial[T^2\setminus\{\mathbf{w}\}]$, $\mathcal{P}|u_a(\mathbf{k})\rangle=\sum_b U_{ab}(\mathbf{k})\big|u_b(\hat{M}\mathbf{k})\rangle$, where $U(\mathbf{k})$ is a unitary matrix acting on the space of the occupied bands, yielding the relation

$$2P_{3} = \frac{i}{24\pi^{2}} \int_{\partial \left[T^{4} \setminus \{\mathbf{w}\}\right]} d^{3}k \hat{n}_{i} \epsilon^{ijkl} \operatorname{tr}\left[\left(U^{\dagger} \partial_{j} U\right) \left(U^{\dagger} \partial_{k} U\right) \left(U^{\dagger} \partial_{l} U\right)\right]. \tag{22}$$

 $2P_3$ is expressed as the winding number of unitary matrix U which has an integer value. We then can prove that

$$v_{4D} = N_1 + \frac{1}{2}N_2 \tag{23}$$

in the presence of parity symmetry near the crossing point. For the massless Wilson fermions, both the first Chern number in 2D and the second Chern number in 4D can be evaluated as a half-integer $-\frac{1}{2} \operatorname{sgn}(b)$.

DATA AVAILABILITY

All data needed to evaluate the conclusions in the paper are present in the paper and/or the Supplementary Materials. Additional data related to this paper may be requested from the authors

Received: 11 April 2022; Accepted: 30 August 2022; Published online: 20 September 2022

REFERENCES

- Klitzing, K. V., Dorda, G. & Pepper, M. New method for high-accuracy determination of the fine-structure constant based on quantized Hall resistance. *Phys. Rev. Lett.* 45, 494–497 (1980).
- 2. Moore, J. E. The birth of topological insulators. Nature 464, 194–198 (2010).
- Hasan, M. Z. & Kane, C. L. Colloquium: topological insulators. Rev. Mod. Phys. 82, 3045–3067 (2010).
- Qi, X.-L. & Zhang, S.-C. Topological insulators and superconductors. Rev. Mod. Phys. 83, 1057–1110 (2011).
- Armitage, N. P., Mele, E. J. & Vishwanath, A. Weyl and Dirac semimetals in threedimensional solids. Rev. Mod. Phys. 90, 015001 (2018).
- Shen, S. Q. Topological insulators. Springer Series of Solid State Science, Vol. 174 (Springer, Heidelberg, 2012).
- Tokura, Y., Yasuda, K. & Tsukazaki, A. Magnetic topological insulators. Nat. Rev. Phys. 1, 126–143 (2019).
- Murakami, S. Phase transition between the quantum spin Hall and insulator phases in 3D: emergence of a topological gapless phase. New J. Phys. 9, 356 (2007).
- Wan, X., Turner, A. M., Vishwanath, A. & Savrasov, S. Y. Topological semimetal and Fermi-arc surface states in the electronic structure of pyrochlore iridates. *Phys. Rev. B* 83, 205101 (2011).

- 10. Soluyanov, A. A. et al. Type-II Weyl semimetals. Nature 527, 495-498 (2015).
- 11. Burkov, A. A., Hook, M. D. & Balents, L. Topological nodal semimetals. *Phys. Rev. B* 84, 235126 (2011).
- Fang, C., Chen, Y., Kee, H.-Y. & Fu, L. Topological nodal line semimetals with and without spin-orbital coupling. *Phys. Rev. B* 92, 081201(R) (2015).
- Bzdušek, T., Wu, Q. S., Rüegg, A., Sigrist, M. & Soluyanov, A. A. Nodal-chain metals. Nature 538, 75–78 (2016).
- Yang, B.-J. & Nagaosa, N. Classification of stable three-dimensional Dirac semimetals with nontrivial topology. *Nat. Commun.* 5, 4898 (2014).
- Schnyder, A. P., Ryu, S., Furusaki, A. & Ludwig, A. W. W. Classification of topological insulators and superconductors in three spatial dimensions. *Phys. Rev. B* 78, 195125 (2008)
- Chiu, C. K., Teo, J. C. Y., Schnyder, A. P. & Ryu, S. Classification of topological quantum matter with symmetries. Rev. Mod. Phys. 88, 035005 (2016).
- Nielsen, H. B. & Ninomiya, M. A no-go theorem for regularizing chiral fermions. *Phys. Lett. B* 105, 219–223 (1981).
- Rothe, H. J. Lattice gauge theories: an introduction. 3rd ed. (World Scientific, Singapore, 2005).
- Wang, H.-W., Fu, B., Zou, J.-Y., Hu, Z.-A. & Shen, S.-Q. Fractional electromagnetic response in three-dimensional chiral anomalous semimetal. *Phys. Rev. B* 106, 045111 (2022).
- Zou, J.-Y., Fu, B., Wang, H.-W., Hu, Z.-A. & Shen, S.-Q. Half-quantized Hall effect and power law decay of edge current distribution. *Phys. Rev. B* 105, L201106 (2022).
- Wilson, K. G. New phenomena in subnuclear physics. ed. A. Zichichi (New York, Plenum. 1975).
- Qi, X.-L., Hughes, T. L. & Zhang, S.-C. Topological field theory of time-reversal invariant insulators. *Phys. Rev. B* 78, 195424 (2008).
- Deser, S., Jackiw, R. & Templeton, S. Topologically massive gauge theories. Ann. Phys. 281, 409–449 (2000).
- Karsten, L. & Smit, J. Lattice Fermions: Species doubling, chiral invariance and the triangle anomaly. *Nucl. Phys. B* 183, 103–140 (1981).
- Adler, S. L. Axial-vector vertex in spinor electrodynamics. Phys. Rev. 177, 2426–2438 (1969).
- 26. Bell, J. S. & Jackiw, R. A PCAC puzzle: $\pi^0 \rightarrow \gamma \gamma$ in the σ -model. *Il Nuovo Cimento A* **60**. 47–61 (1969).
- Niemi, A. J. & Semenoff, G. W. Axial-anomaly-induced fermion fractionization and effective gauge-theory actions in odd-dimensional space-times. *Phys. Rev. Lett.* 51, 2077–2080 (1983).
- Haldane, F. D. M. Model for a quantum Hall effect without Landau levels: condensedmatter realization of the "parity anomaly". Phys. Rev. Lett. 61, 2015–2018 (1988).
- 29. Hatcher, A. Algebraic topology (Cambridge University Press, Cambridge, 2002).
- Mermin, N. D. The topological theory of defects in ordered media. Rev. Mod. Phys. 51, 591–648 (1979).
- Altland, A. & Zirnbauer, M. R. Nonstandard symmetry classes in mesoscopic normal-superconducting hybrid structures. *Phys. Rev. B* 55, 1142–1161 (1997).
- Berry, M. V. Quantal phase factors accompanying adiabatic changes. Proc. R. Soc. A Math. Phys. Eng. Sci. 392, 45–57 (1984).
- 33. Resta, R. Theory of the electric polarization in crystals. Ferroelectrics 136, 51–55 (1992).
- King-Smith, R. D. & Vanderbilt, D. Theory of polarization of crystalline solids. Phys. Rev. B 47, 1651–1654 (1993).
- Nayak, C., Simon, S. H., Stern, A., Freedman, M. & Sarma, S. D. Non-Abelian anyons and topological quantum computation. Rev. Mod. Phys. 80, 1083–1159 (2008).
- Xiao, D., Chang, M.-C. & Niu, Q. Berry phase effects on electronic properties. Rev. Mod. Phys. 82, 1959–2007 (2010).
- Wilczek, F. & Zee, A. Appearance of gauge structure in simple dynamical systems. Phys. Rev. Lett. 52, 2111–2114 (1984).
- Zhang, S. L. & Zhou, Q. Two-leg Su-Schrieffer-Heeger chain with glide reflection symmetry. Phys. Rev. A 95, 061601(R), (2017).
- 39. Thouless, D. J. Quantum of particle transport. Phys. Rev. B 27, 6083-6087 (1983).
- Niu, Q. Towards a quantum pump of electric charges. Phys. Rev. Lett. 64, 1812–1815 (1990).
- Nakajima, S. et al. Topological Thouless pumping of ultracold fermions. *Nat. Phys.* 12, 296–300 (2016).
- Lohse, M. et al. A Thouless quantum pump with ultracold bosonic atoms in an optical superlattice. Nat. Phys. 12, 350–354 (2016).
- Crowley, P. J. D., Martin, I. & Chandran, A. Half-integer quantized topological response in quasiperiodically driven quantum system. *Phys. Rev. Lett.* 125, 100601 (2020).
- Hatsugai, Y. Chern number and edge states in the integer quantum Hall effect. Phys. Rev. Lett. 71, 3697–3700 (1993).
- Chu, R. L., Shi, J. R. & Shen, S. Q. Surface edge state and half-quantized Hall conductance in topological insulators. *Phys. Rev. B* 84, 085312 (2011).
- Jackiw, R. & Rebbi, C. Solitons with fermion number 1/2. Phys. Rev. D 13, 3398–3409 (1976).
- Fradkin, E. Field theories of condensed matter physics (Cambridge University Press, 2013).



- 48. Böttcher, J., Tutschku, C., Molenkamp, L. W. & Hankiewicz, E. M. Survival of the quantum anomalous Hall effect in orbital magnetic fields as a consequence of the parity anomaly. Phys. Rev. Lett. 123, 226602 (2019).
- 49. Burkov, A. A. Dirac fermion duality and the parity anomaly. Phys. Rev. B 99, 035124
- 50. Callan, C. G.Jr. & Harvey, J. V. Anomalies and fermion zero modes on strings and domain walls. Nucl. Phys. B 250, 427-436 (1985).
- 51. Wen, X. G. Gapless boundary excitations in the quantum Hall states and in the chiral spin states. Phys. Rev. B 43, 11025-11036 (1991).
- 52. Büttner, B. et al. Single valley Dirac fermions in zero-gap HgTe quantum wells.
- Nat. Phys. 7, 418-422 (2011). 53. Mutch, J. et al. Evidence for a straintuned topological phase transition in ZrTes,
- Sci. Adv. 5, eaav9771 (2019). 54. Elcoro, L. et al. Magnetic topological quantum chemistry. Nat. Commun. 12, 5965 (2021)
- 55. Chernodub, M. N. The Nielsen-Ninomiya theorem, PT-invariant non-Hermiticity and single 8-shaped Dirac cone. J. Phys. A 50, 385001 (2017).
- 56. Mogi, M. et al. Experimental signature of parity anomaly in semi-magnetic topological insulator. Nat. Phys. 18, 390-394 (2022).
- 57. Ryu, S., Schnyder, A. P., Furusaki, A. & Ludwig, A. W. W. Topological insulators and superconductors: tenfold way and dimensional hierarchy. New J. Phys. 12, 065010 (2010).

ACKNOWLEDGEMENTS

This work was supported by the Research Grants Council, University Grants Committee, Hong Kong under Grant Nos. C7012-21G and 17301220, and the National Key R&D Program of China under Grant No. 2019YFA0308603.

AUTHOR CONTRIBUTIONS

All authors contributed to performing the calculations and the analysis of the results. S.Q.S. was responsible for the supervision of the project. S.Q.S. and B.F. wrote the manuscript with suggestions from all authors.

COMPETING INTERESTS

The authors declare no competing interests.

ADDITIONAL INFORMATION

Supplementary information The online version contains supplementary material available at https://doi.org/10.1038/s41535-022-00503-0.

Correspondence and requests for materials should be addressed to Shun-Qing Shen.

Reprints and permission information is available at http://www.nature.com/ reprints

Publisher's note Springer Nature remains neutral with regard to jurisdictional claims in published maps and institutional affiliations.

Open Access This article is licensed under a Creative Commons Attribution 4.0 International License, which permits use, sharing,

adaptation, distribution and reproduction in any medium or format, as long as you give appropriate credit to the original author(s) and the source, provide a link to the Creative Commons license, and indicate if changes were made. The images or other third party material in this article are included in the article's Creative Commons license, unless indicated otherwise in a credit line to the material. If material is not included in the article's Creative Commons license and your intended use is not permitted by statutory regulation or exceeds the permitted use, you will need to obtain permission directly from the copyright holder. To view a copy of this license, visit http:// creativecommons.org/licenses/by/4.0/.

© The Author(s) 2022